



Article

# Effect of Humidity on CO<sub>2</sub>/N<sub>2</sub> and CO<sub>2</sub>/CH<sub>4</sub> Separation Using Novel Robust Mixed Matrix Composite Hollow Fiber Membranes: Experimental and Model Evaluation

Clara Casado-Coterillo , Ana Fernández-Barquín and Angel Irabien 

Department of Chemical and Biomolecular Engineering, Universidad de Cantabria, s/n, 39005 Santander, Spain; fbarquina@unican.es (A.F.-B.); irabienj@unican.es (A.I.)

\* Correspondence: casadoc@unican.es; Tel.: +34-942-20-6777

Received: 29 November 2019; Accepted: 23 December 2019; Published: 30 December 2019



**Abstract:** In this work, the performance of new robust mixed matrix composite hollow fiber (MMCHF) membranes with a different selective layer composition is evaluated in the absence and presence of water vapor in CO<sub>2</sub>/N<sub>2</sub> and CO<sub>2</sub>/CH<sub>4</sub> separation. The selective layer of these membranes is made of highly permeable hydrophobic poly(trimethyl-1-silylpropine) (PTMSP) and hydrophilic chitosan-ionic liquid (IL-CS) hybrid matrices, respectively, filled with hydrophilic zeolite 4A particles in the first case and HKUST-1 nanoparticles in the second, coated over compatible supports. The effect of water vapor in the feed or using a commercial hydrophobic PDMSXA-10 HF membrane has also been studied for comparison. Mixed gas separation experiments were performed at values of 0 and 50% relative humidity (RH) in the feed and varying CO<sub>2</sub> concentration in N<sub>2</sub> and CH<sub>4</sub>, respectively. The performance has been validated by a simple mathematical model considering the effect of temperature and relative humidity on membrane permeability.

**Keywords:** mixed matrix; composite hollow fiber membrane; CO<sub>2</sub> separation; humid gas streams; modeling validation

## 1. Introduction

Membrane technology for CO<sub>2</sub> separation from other gases, especially N<sub>2</sub> and CH<sub>4</sub>, faces challenges to upgrade to large scale, partly due to the uncertainty of the behavior in the presence of impurities such as water vapor in real gas separation [1–6], and partly to the trade-off between permeability and selectivity in a gas pair separation that has been often proposed to be overcome by emerging materials [7]. Among these, mixed matrix membranes (MMMs) combine the processability of polymers with the molecular sieving effect of inorganic fillers, and have been investigated intensively for light gas separation [8]. Despite the achievements carried out in material development in the last decades at lab scale, there is still a gap between lab and practical conditions because of the difficulty of fabrication of membranes from new materials [9]. Multilayer composite membranes offer the possibility to optimize membrane layer materials independently and reduce the overall transport resistance by coating ultrathin highly selective and permeable layers on mechanically robust and processable supports [10].

This way, a multilayer composite hollow fiber (CHF) approach allows the transfer of the selective layer properties to other geometries [11], which could be more easily implemented at a large scale, by dip-coating the selective material as a thin layer on a robust support, which is simpler than wet-dry phase inversion spinning [12,13], co-extruding a thin ion-exchange hydrophilic polymer high performance material on hydrophobic polysulfone (PSf) [14], or growing zeolites in a polymer

support [15]. One of the most important impurities in CO<sub>2</sub> separation is water vapor because the relative humidity of the feed gas [16]. It has been suggested that water vapor can affect the membrane performance differently depending on the hydrophobic or hydrophilic character of the selective layer material and the affinity of H<sub>2</sub>O with the gas penetrants [17,18]. If the membrane is hydrophobic, water has been reported to reduce the solubility of gases through competitive effects, lower the free volume of the polymer or reduce diffusivity by blocking effects of the pores of hydrophilic pores in MMMs [19]. If the membrane were hydrophilic, the interaction with water can be strong and increasing when exposed to humid conditions, the gas permeance being due to the increased gas diffusivity [20]. This can be prevented by coating a layer of a different character on top of the composite membrane, the support, or by combining hydrophilic and hydrophobic components in the selective layer [21].

Defects that make the membrane unselective also need to be controlled [22], but intrusion of the coated layer in the pores of the support has to be avoided to maintain the high flux needed in CO<sub>2</sub> separation. This has been attempted by pre-wetting the substrate in water [17], adding a hydrophobic gutter layer of polydimethylsiloxane (PDMS) [23], or poly(trimethyl silyl-1-propyne) (PTMSP) between a hybrid hydrophilic selective layer and the porous support [24,25], or coating a protective layer of a high free volume AF2400 [22] or hydrophilic chitosan (CS) biopolymer [26,27] on porous hydrophilic substrates to simultaneously enhance both permeance and selectivity in CO<sub>2</sub> separation.

In this work, we study the experimental separation of CO<sub>2</sub>/N<sub>2</sub> and CO<sub>2</sub>/CH<sub>4</sub> mixtures in dry and wet conditions, as a function of feed concentration and the composition of the selective layer of hydrophobic PTMSP/P84 and hydrophilic IL-CS/PSf composite hollow fiber (CHF) membranes, both highly CO<sub>2</sub> permeable and thermally robust polymers. The selective layer has also been modified by the MMM concept, using compatible fillers that enhanced the permselectivity and mechanical resistance of the pure polymer materials [28,29], such as HKUST-1-IL-CS and Zeolite 4A-PTMSP MMMs, even when transferred to hollow fiber geometry at increasing operating temperatures by an appropriate choice of compatible selective layer components and supports [30], to create mixed matrix composite hollow fiber (MMCHF) membranes. The separation performance of these membranes was evaluated in this work by the adaptation of a simple mathematical model developed previously for the CO<sub>2</sub>/N<sub>2</sub> separation as a function of temperature, concentration, and number of membrane modules in series [31].

## 2. Materials and Methods

The preparation and morphological characterization of the CHF and MMCHF membranes studied here was presented in a previous work [30]. PTMSP and 20 wt.% zeolite A-PTMSP MMCHF membranes were prepared by coating the selective solution on the outer side of a P84 HF support, with the ends covered to prevent penetration in the lumen side. Likewise, IL-CS and 5 wt.% HKUST-1 MMCHF membranes were prepared on the outer side of a PSf HF support. In order to do these, PTMSP was purchased from ABCR (Karlsruhe, Germany), CS, IL and Zeolite 4A from Aldrich (Madrid, Spain), while HKUST-1 nanoparticles were supplied by the University of Zaragoza [29] and the P84 and PSf HF supports by Tecnalia [30].

The performance of the membranes for the separation of CO<sub>2</sub>/N<sub>2</sub> and CO<sub>2</sub>/CH<sub>4</sub> mixtures was experimentally evaluated in a home-made separation setup at 0% and 50% relative humidity (RH) (Figure 1). To perform the wet gas experiments, the feed gas at the operating pressure and temperature was half-passed through a water tank, as shown in the Figure 1, before being introduced to the shell side of the hollow fiber membranes. The stop valves in Figure 1 prevented the entrance of liquid water to the membrane module, allowing comparison of the behavior of the membrane in the presence and absence of water vapor [32]. A commercial PDMSXA-10 HF membrane (Permsilicone<sup>®</sup>) has also been tested for comparison purposes. The membrane modules can be seen in the photographs in Figure 2, where Figure 2a is the commercial module and Figure 2b the module where the lab-made CHF and MMCHF membranes were placed for testing. The experiments were performed at room temperature (293K) and 4.5 bar absolute feed pressure, commonly encountered conditions in the characterization of

MMMs and thin-film composite (TFC) membranes for CO<sub>2</sub> separation reported in literature [20,33–35]. The sequence of experiments conducted in the separation plant is presented in Table 1.

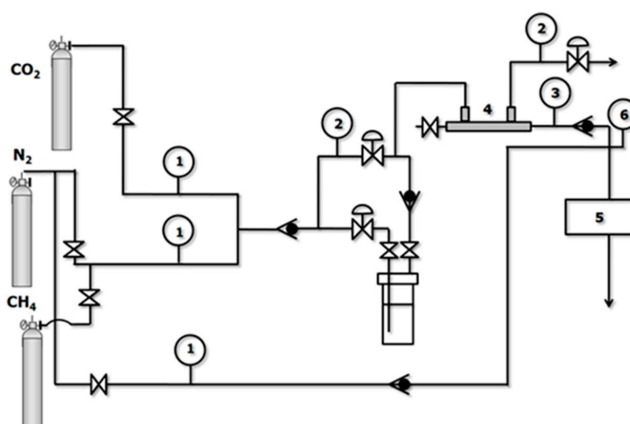


**Figure 1.** Experimental setup. (1) Mass flow meters, (2) pressure regulators, (3) pressure gauges, (4) HF membrane module, (5) analyzer, (6) bubble flowmeter.



(a)



(b)

**Figure 2.** Photographs of the commercial PDMSXA-10 HF membrane module and the home-made stainless-steel modules used to measure the separation performance of the CHF and MMCHF membranes in our laboratory.

**Table 1.** Sequence of CO<sub>2</sub> separation experiments conducted for each membrane.

Experiment <sup>1</sup>	CO <sub>2</sub> (wt.%)	N <sub>2</sub> (wt.%)	CH <sub>4</sub> (wt.%)	RH (%)
1	0	100	0	0
2	0	0	100	0
3	25	75	0	0
4	25	0	75	0
5	50	50	0	0
6	50	0	50	0
7	75	25	0	0
8	75	0	25	0
9	100	0	0	0
10	0	100	0	50
11	0	0	100	50
12	25	75	0	50
13	25	0	75	50
14	50	50	0	50
15	50	0	50	50
16	75	25	0	50
17	75	0	25	50
18	100	0	0	50

<sup>1</sup> Noteworthy were the order of gas concentrations (N<sub>2</sub>, CH<sub>4</sub>, CO<sub>2</sub>) and dry and wet streams in order to assure reproducibility of the membrane materials between experiments, as reported elsewhere [18].

Once the membrane performance reached a steady state, the permeate was measured using a bubble flow meter at the end of the system (6) at least 3 times over for about 1 h to confirm the

membrane stability at a given operating condition. Stable performance was attained after 3 h in dry conditions. The composition of the permeate was determined by a gas analyzer (BIOGAS5000, Geotech, USA, purchased from Fonotest S.L., Madrid, Spain).

The permeance of gas  $i$ , was calculated as

$$\left(\frac{P_i}{t}\right) = \frac{Q \times y_i}{A \Delta p_i} \quad (1)$$

Permeance is expressed as usual in terms of GPU (1 GPU =  $10^{-6}$  cm<sup>3</sup> (STP) cm<sup>-2</sup> s<sup>-1</sup> cmHg<sup>-1</sup>), where  $i$  is referred to the permeating gas molecule,  $\Delta p_i$  the partial pressure difference for the gas component  $i$  across the membrane,  $A$  the effective area of the membrane,  $t$  the effective layer thickness for the separation and  $Q$  the permeate flow rate (cm<sup>3</sup>/s) at measurement pressure and temperature conditions. The effective area of the MMCHF membranes was 2.2 cm<sup>2</sup>. The effective area of the commercial PDMSXA-10 HF membrane was 10 cm<sup>2</sup>, the smallest we have found to compare with the lab-made MMCHF membranes.

The selectivity was calculated as the ratio between the permeance of the fast gas  $i$ , i.e., CO<sub>2</sub>, and the slow gas,  $j$ , in this work, N<sub>2</sub> or CH<sub>4</sub>, respectively, as expressed by

$$\beta_{ij} = \frac{(P/t)_i}{(P/t)_j} \quad (2)$$

where  $P$  is the intrinsic selective material permeability measured by single gas permeation through the self-standing materials in previous works [28,29],  $t$  the effective layer thickness, taken from the previous work as  $0.5 \pm 0.1$ ,  $1.9 \pm 0.5$ ,  $7.2 \pm 1.7$  and  $6.9 \pm 1.5$  μm, for IL-CS/PSf, 5wt.% HKUST-1-IL-CS/PSf, PTMSP/P84 and 20 wt.% zeolite A-PTMSP/P84 membranes, respectively. These data are reported in a previous work [30].

The influence of membrane composition, type of separation and feed concentration on the separation performance have been evaluated experimentally and validated a simple mathematical model developed in a previous work using Aspen Custom Modeler® [31]. On the one hand, this model has been updated in this work to take into account the change of geometry by updating the model assumptions as in [36] for thermally resistant hollow fiber membranes:

- ideal gas behavior,
- no deformation of the hollow fiber or gas leakage losses,
- the inner and outer diameters and of the hollow fibers thickness of the selective layer are uniform for the whole effective length of the module,
- the effect of concentration polarization is negligible,
- the permeance depends on the feed conditions, and can be estimated based on correlations dependent on conditions including pressure, flowrate, and composition, and
- the pressure drop is negligible on both the permeate and feed sides [37].

Furthermore, the effect of the selective layer and support is taken into account using the resistance-in-series approach [38–40], as

$$\left(\frac{t}{P}\right)_{global} = \left(\frac{t}{P}\right)_{support} + \left(\frac{t}{P}\right)_{selective\ layer} \quad (3)$$

On the other hand, the model has been also updated to account for the effect of humidity by using the NELF-based solubility-diffusivity approach with two adjustable parameters A and B depending on the selective membrane material properties for each penetrating gas molecule, as [21,41].

$$P(a) = D(a) \cdot S(a) = A \cdot \exp\left(\frac{-B}{FFV(a)}\right) \cdot S(a) \quad (4)$$

where  $FFV(a)$  is the fraction of free volume available for gas transport as a function of the water activity,  $a$ , in the system, which accounted for the presence of water vapor in the feed. The values of  $A$  and  $B$  for PTMSP and Zeolite A-PTMSP MMM were reported elsewhere [21], and those used for IL-CS and HKUST-1/IL-CS MMM were estimated from the permeability values measured in the laboratory in wet and dry conditions.

### 3. Results and Discussion

#### 3.1. Experimental Evaluation

The experimental results of the  $\text{CO}_2/\text{N}_2$  and  $\text{CO}_2/\text{CH}_4$  gas mixture separations in dry and wet conditions for the different membranes are discussed in the following lines.

The separation performance through the commercial PDMS10XA-10 HF membrane is shown in Figure 3. The  $\text{CO}_2$  permeance through this rubbery hydrophobic membrane increased with increasing  $\text{CO}_2$  content in the feed mixture, while the  $\text{N}_2$  and  $\text{CH}_4$  permeances did not decrease. The reduction of the low permeating gas ( $\text{N}_2$ ,  $\text{CH}_4$ ) permeance was less significant than that of  $\text{CO}_2$ , due to differences in condensability (boiling point of  $\text{N}_2$  77 K,  $\text{CH}_4$ , 112 K and  $\text{CO}_2$ , 126 K) and kinetic diameter (0.38 nm, 0.34 and 0.33 nm, for  $\text{CH}_4$ ,  $\text{N}_2$  and  $\text{CO}_2$ , respectively). Thus, the differences of  $\text{CO}_2/\text{CH}_4$  and  $\text{CO}_2/\text{N}_2$  selectivities in Figure 3b, may be attributed to competing and synergistic interactions between the penetrants and the polymer selective layer. The presence of water vapor, reduced the  $\text{CO}_2/\text{N}_2$  selectivity more than the  $\text{CO}_2/\text{CH}_4$  selectivity, as observed in Figure 3b, because the slow gas permeance decreased at increasing  $\text{CO}_2$  concentration in the feed, due to the favorable competition for adsorption coverage sites in the membrane matrix. Therefore, the selectivity generally increased in the presence of water vapor, i.e., up to around 40% in the case of  $\text{CO}_2/\text{N}_2$  selectivity, in agreement with the partial recovery of the slow gas permeance recovered after a series of experiments in the presence of water vapor, as observed by Chenar et al. [18] for commercial polymer HF membranes.

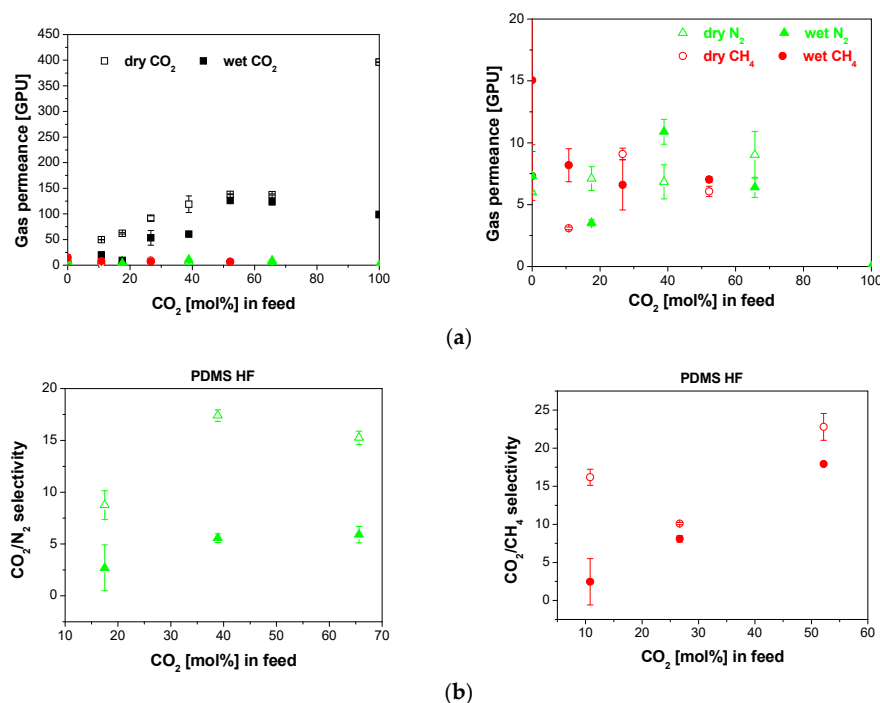


**Figure 3.** Gas permeance (a) and selectivity (b) obtained for the separation of  $\text{CO}_2/\text{N}_2$  (left) and  $\text{CO}_2/\text{CH}_4$  (right) mixtures through the commercial PDMSXA-10 HF membrane in dry (void symbols) and wet (full symbols). The right side of figure (a) shows the trend in the slow gas ( $\text{N}_2$ ,  $\text{CH}_4$ ) permeance.

In Figure 4 the CO<sub>2</sub>/N<sub>2</sub> and CO<sub>2</sub>/CH<sub>4</sub> mixtures separation performance in the absence and presence of water vapor the PTMSP/P84 CHF membranes prepared in the laboratory, is presented. Similar to the commercial PDMSXA-10 HF membrane in Figure 3, the presence of water vapor in the gas stream hardly decreases the CO<sub>2</sub> permeance or the selectivity of the PTMSP/P84 CHF membrane in Figure 4. This was again attributed to the combined effect between competitive sorption and transport, perhaps due to the high free volume and rigid structure of PTMSP [18,19]. The selectivity values in Figure 4b were of the same order of magnitude as other PTMSP/P84 CHF membranes reported in literature [19]. Since the gas permeance and selectivity were not altered by the presence of water vapor, it was expected that the integrity of the polymer coating was preserved through the experiments [42]. This observation agreed with other authors' results on membranes coated with PDMS to prevent the water molecules being trapped in the hydrophilic support [19]. When those membranes showed the same performance wet as dry [30], this was considered as an indication of the defect ratio of the CHF membrane [22].

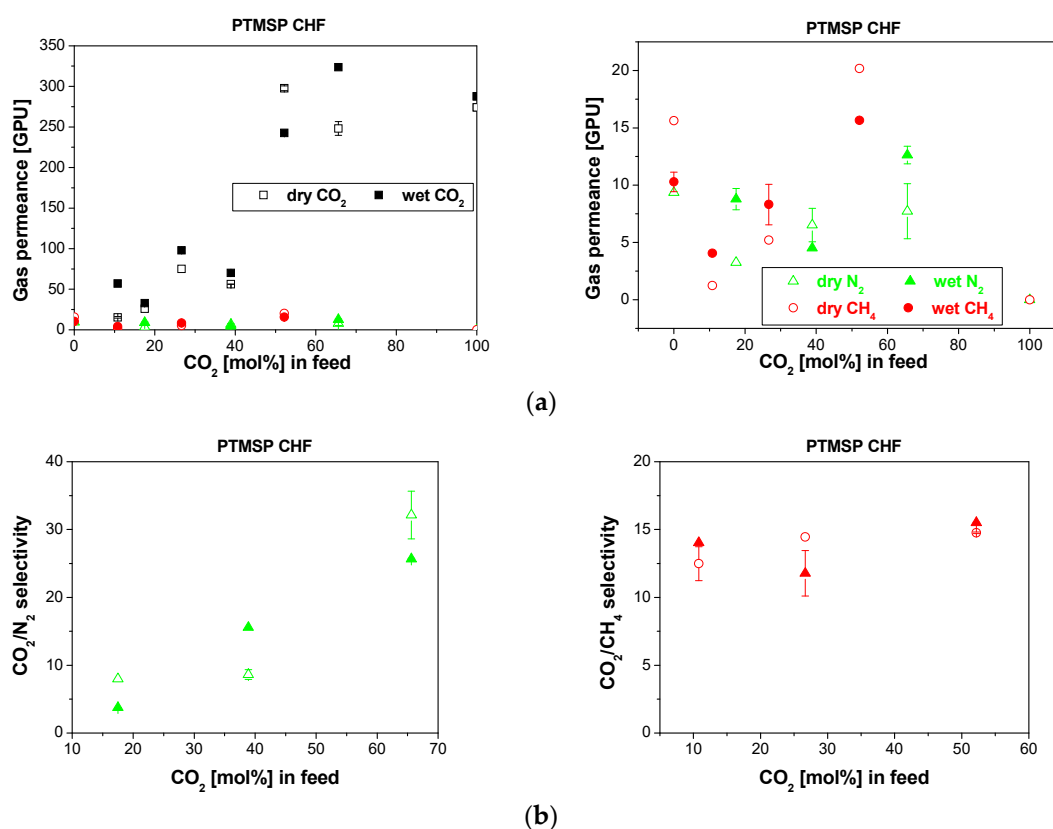


**Figure 4.** Gas permeance (a) and selectivity (b) obtained for the separation of CO<sub>2</sub>/N<sub>2</sub> (left) and CO<sub>2</sub>/CH<sub>4</sub> (right) mixtures through the PTMSP/P84 CHF membrane in dry (void symbols) and wet (full symbols). The right side of figure (a) shows the trend in the slow gas (N<sub>2</sub>, CH<sub>4</sub>) permeance.

The behavioral trend observed in Figures 3 and 4 was opposed to that of the IL-CS/PSf CHF membrane in Figure 5, where the presence of water vapor in the feed increased the CO<sub>2</sub> permeance while diminishing the fluxes of CH<sub>4</sub> and N<sub>2</sub>, probably because of swelling of the IL-CS matrix, thus revealing the hydrophilic nature of the selective IL-CS layer [29].



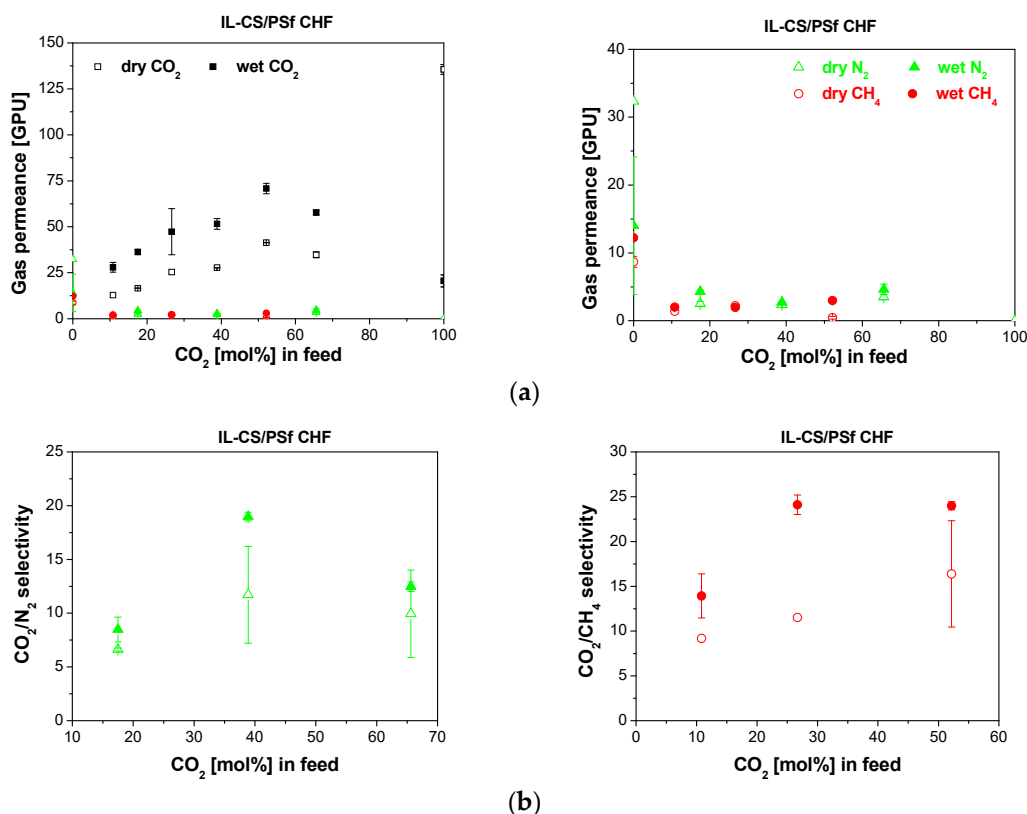


**Figure 5.** Gas permeance (a) and selectivity (b) obtained for the separation of CO<sub>2</sub>/N<sub>2</sub> (left) and CO<sub>2</sub>/CH<sub>4</sub> (right) mixtures through the IL-CS/PSf CHF membrane in dry (void symbols) and wet (full symbols). The right side of figure (a) shows the trend in the slow gas (N<sub>2</sub>, CH<sub>4</sub>) permeance.

Although the selectivity through the hydrophilic IL-CS/PSf membrane increased at low CO<sub>2</sub> concentration in the feed by the effect of water vapor, for CO<sub>2</sub>/N<sub>2</sub> and CO<sub>2</sub>/CH<sub>4</sub> separation, the selectivity declined at higher concentration probably because of the carrier effect of CO<sub>2</sub> and water through the membrane [43]. Highly hydrophilic membranes have been observed to interact strongly with water vapor, causing a drop in the performance in wet compared to dry conditions [35]. This is even more remarked at increasing CO<sub>2</sub> feed concentration because of the interaction of CO<sub>2</sub> with water molecules [33].

In fact, the hydrophilic IL-CS/PSf CHF shows a slight increase of CO<sub>2</sub> selectivity and CO<sub>2</sub> permeance in the presence of water vapor conditions, compared to dry, at 25 wt.% CO<sub>2</sub> feed concentration, which may be attributed to the role of the [emim][Ac] ionic liquid in the selective layer upon wet gas permeation experiments, as reported elsewhere [35]. Fam et al. controlled the swelling of Pebax-IL CHF membranes by adding graphene oxide (GO) sheets with high water affinity [20]. In our laboratory, we attempted doing so by adding nanoparticles with high water and CO<sub>2</sub> affinity [44,45]. Thus, as previously reported [29], the IL is also acting as a binder or void filler [46] with the HKUST-1 nanoparticles in the selective layer of 5 wt.% HKUST-1-IL-CS/PSf MMCHFs, leading to higher increases in CO<sub>2</sub> permeance and selectivity than those observed for the rest of the MMCHF membranes in this work. This agrees with the observations reported for thermally arranged HF membranes on the separation of simulated flue gas mixtures [47], and it may be attributed to the combined hydrophilic and hydrophobic nature of the selective membrane layer and the successful coating of the effective length of the support, providing a lower defect ratio [17].

The experimental results of the CO<sub>2</sub> separation performance through our HKUST-1-IL-CS/PSf MMCHF membranes are plotted in Figure 6. Interestingly, the CO<sub>2</sub> permeance through the HKUST-1/IL-CS MMCHF membrane in Figure 6a increased dramatically compared to the IL-CS/PSf HF membrane in Figure 5a, and although the CO<sub>2</sub> permeance decreased slightly in wet CO<sub>2</sub>/N<sub>2</sub> separation,

compared to dry conditions, the values of these membranes were the highest obtained for all the membranes reported in this work.

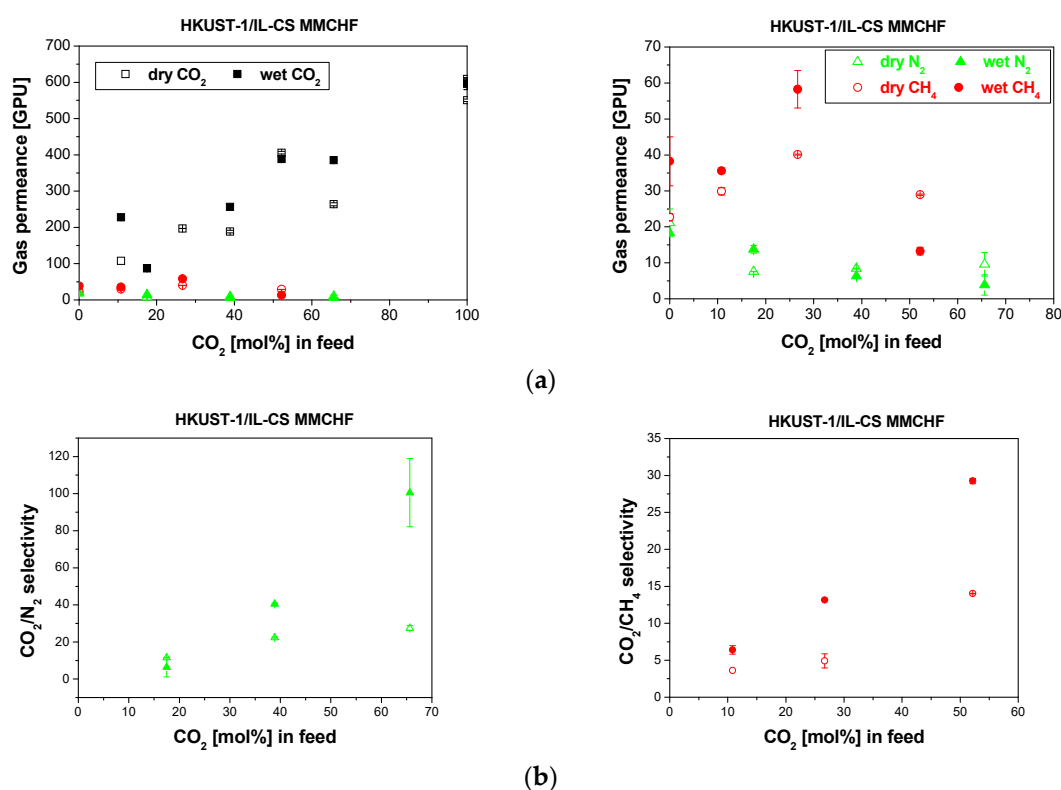


**Figure 6.** Gas permeance (a) and selectivity (b) obtained for the separation of CO<sub>2</sub>/N<sub>2</sub> (left) and CO<sub>2</sub>/CH<sub>4</sub> (right) mixtures through the HKUST-1/IL-CS/PSf MMCHF membrane in dry (void symbols) and wet (full symbols). The right side of figure (a) shows the trend in the slow gas (N<sub>2</sub>, CH<sub>4</sub>) permeance.

The selectivity of the membranes is increased from 10–20 for the polymer IL-CS/PSf CHF in Figure 5, to 40–50 for the MMCHF in Figure 6. This values are in agreement with other MMCHF membranes reported in literature, as observed by other authors for hydrophilic amine-modified SAPO-34-IL/Pebax-PEGDME MMCHF [46], or GO-IL/PTMSP/PVDF MMCHF [20], in 20:80 (%) CO<sub>2</sub>:N<sub>2</sub> and CO<sub>2</sub>:CH<sub>4</sub> mixture separation, and thereby attributed to the competitive sorption between CH<sub>4</sub> and CO<sub>2</sub>.

Hydrophilic zeolite fillers and hydrophilic glassy polymers usually have to be surface-modified to increase their compatibility. The combination of hydrophilic zeolite fillers and hydrophobic polymer matrices in the selective layer influenced the CO<sub>2</sub> permeance and selectivity of Zeolite A/PTMSP MMMs in the presence of water vapor [21], and is appreciated for the Zeolite A-PTMSP/P84 MMCHF in Figure 7. This was attributed to the effect of the introduction of the zeolite A particles in the PTMSP matrix [21], by simultaneously influencing the plasticization of the PTMSP polymer and the water sorption and molecular sieving of the zeolite A. The water uptake was increased from 9.5 ± 5% for PTMSP to 33 ± 6% for the 20 wt.% Zeolite A-PTMSP MMM. This was the cause of the decrease in CO<sub>2</sub> permeance in wet conditions. The N<sub>2</sub> and CH<sub>4</sub> permeance were less influenced by water vapor presence than they were for the hydrophobic PTMSP/P84 CHF and PDMSXA-10 HF membranes, and so the CO<sub>2</sub>/N<sub>2</sub> and CO<sub>2</sub>/CH<sub>4</sub> selectivity increased around 34% and 46%, respectively, from dry to humid conditions.



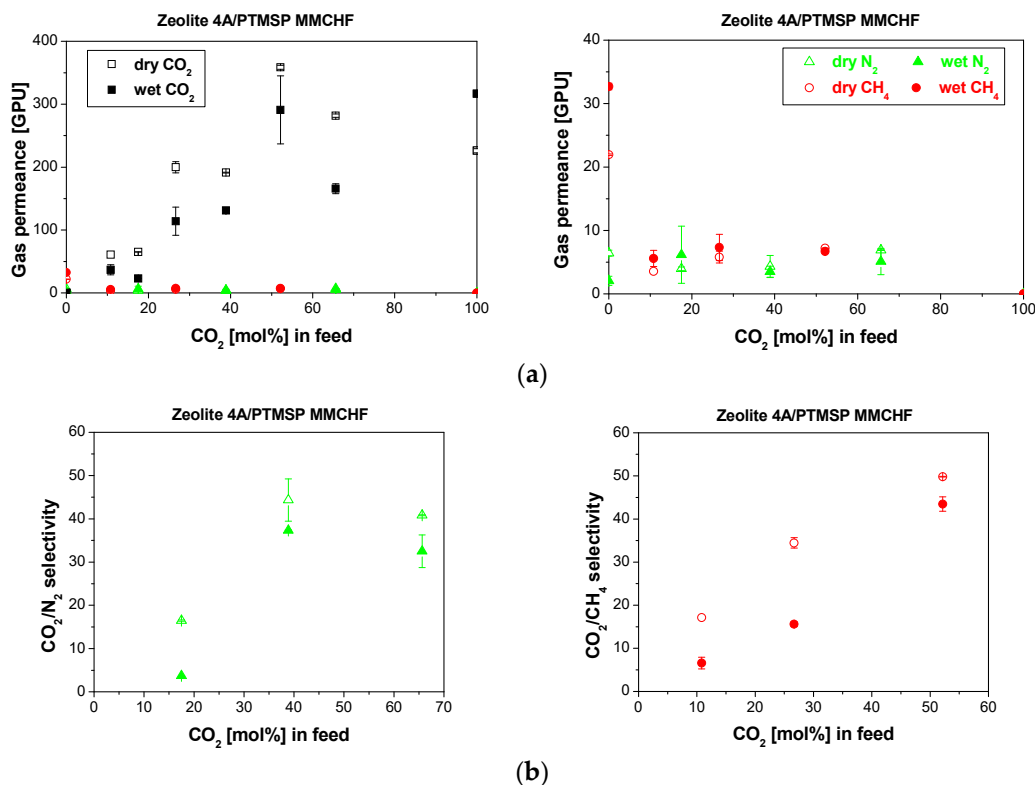


**Figure 7.** Gas permeance (a) and selectivity (b) obtained for the separation of CO<sub>2</sub>/N<sub>2</sub> (left) and CO<sub>2</sub>/CH<sub>4</sub> (right) mixtures through the Zeolite A/PTMSP/P84 MMCHF membrane in dry (void symbols) and wet (full symbols). The right side of figure (a) shows the trend in the slow gas (N<sub>2</sub>, CH<sub>4</sub>) permeance.

In the feed. The combination of hydrophilic Zeolite A and PTMSP in the selective layer of the composite membrane provided a stable performance at 25 wt.% CO<sub>2</sub> concentration in the feed. Especially, the constant value of CO<sub>2</sub> permeance at high CO<sub>2</sub> concentration reached in CO<sub>2</sub>/CH<sub>4</sub> separation, may be correlated to the robustness of the 20 wt.% Zeolite A-PTMSP/P84 MMCHF membrane, attributed to the compatibility of the membrane materials components [30] without needing surface modification of the zeolites [48].

### 3.2. Model Validation

The agreement with the model used in this work is a function of the type of selective membrane material. For the commercial PDMSXA-10, it was acceptable, except at high CO<sub>2</sub> concentration in the feed. There, the deviations can be attributed to the plasticizing effect by CO<sub>2</sub> and the competing and synergistic interaction between the penetrants and the polymer matrix that is the base component of the selective layer of a composite membrane, causing a decrease in slow gas permeance at increasing CO<sub>2</sub> concentration [18,49].

The calculated permeance of the MMCHF takes into account the consideration of the presence of water vapor in the feed, by introducing the Equation (4) obtained in a previous work [21], into the model.

The model prediction for this work CHF membranes is more accurate than in the case of the commercial PDMSXA-10 HF membrane, probably because it has been easier to consider the resistance in series of the different layers by Equation (3) and the effect of plasticization is not as significant as that of water vapor [49–51], given the low pressure difference of the separation experiments (75 psi in the feed side and 15 psi in the permeate side) [37].

The experimental results were validated by the simple mathematical model incorporating Equations (3) and (4) to account for the change of geometry and the effect of humidity in the feed.

The parity plots in Figure 8 show that this model predicts the  $\text{CO}_2/\text{N}_2$  performance in dry conditions better, with an error below 20% (lines in Figure 8), while the  $\text{CO}_2/\text{CH}_4$  behavior of the membranes is validated only in the presence of water vapor, with large deviations in dry conditions, as shown in the left-handed Figure 8a. The error in the  $\text{CO}_2$  permeate flux is also lower in wet than dry conditions, especially when the hydrophilicity of the selective CHF membrane can be tuned up [33].

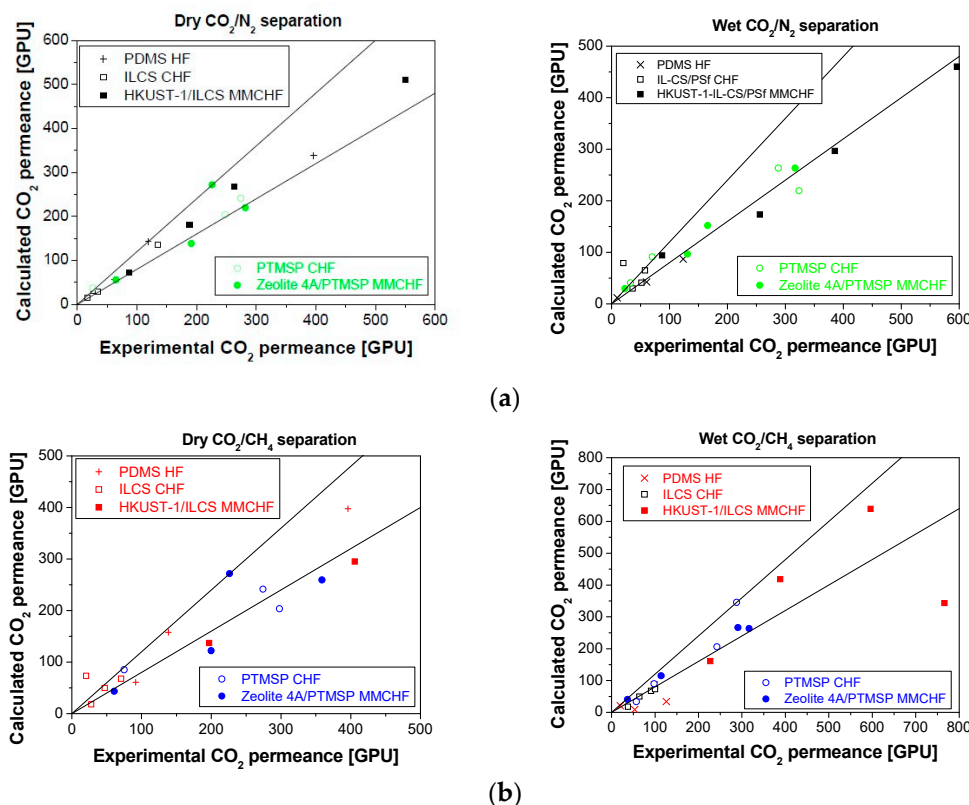


**Figure 8.** Parity plots for the  $\text{CO}_2$  permeance in dry (left) and humid conditions (right) obtained for the  $\text{CO}_2/\text{N}_2$  (a) and  $\text{CO}_2/\text{CH}_4$  (b) separation for all membranes tested in this work.

The influence of water vapor in the feed stream on the permeation flux depends on the hydrophobic or hydrophilic character of the selective layer of the membrane, as this facilitates the affinity towards  $\text{CO}_2$  [45]. On the one hand, the permeance through the PDMSXA-10 and PTMSP membranes decreased in wet conditions, in response to the competitive sorption and transport through the hydrophobic membranes. On the other hand, the  $\text{CO}_2$  permeance through the IL-CS/PSf membrane increased in the presence of water vapor, with increasing  $\text{CO}_2$  concentration in the feed, which may be attributed to the increasing hydrophilic character of the selective layer [29].

The influence of water on  $\text{CO}_2$  solubility has been observed to alter the performance of other glassy polymer based MMMs [52]. Thus this model can still be enhanced in the future by considering recent advances taking into account the interfacial layer distance and distribution of the particles in the polymer matrix [53], as well as the water activity introduced in this work by Equation (4), in order to improve the accuracy of the model.

#### 4. Conclusions

The experimental  $\text{CO}_2$  permeance and selectivity on the separation of  $\text{CO}_2/\text{N}_2$  and  $\text{CO}_2/\text{CH}_4$  mixtures, using several hollow fiber membranes, was measured in the absence and presence of water vapor in the feed. On the one hand, the permeance through the PDMSXA-10 HF and the PTMSP CHF membranes decreased in wet conditions in response to the competitive sorption and transport through the hydrophobic membranes. On the other hand, the  $\text{CO}_2$  permeance through the IL-CS/PSf

membrane increased in the presence of water vapor, with increasing CO<sub>2</sub> concentration in the feed. This was also observed for the HKUST-1-IL-CS/PSf and the zeolite A-PTMSP/P84 MMCHF membranes, which accounts for the possibility to tune up the CO<sub>2</sub> separation by altering the hydrophilicity of the selective layer material in composite membranes. The experimental results have been validated by a simple mathematical model, adding the effect of the hollow fiber geometry and the influence of water activity in the gas feed, with a global error generally lower than 20%.

This work provides scope for the evaluation of novel CHF membranes in CO<sub>2</sub> separation processes with non-ideal mixtures, to fill in the existing gap from laboratory to bench scale in the presence of impurities. Further characterization of the CO<sub>2</sub> separation performance at higher pressures and in the presence of other impurities such as hydrocarbons in the absence and presence of water vapor conditions [51], both experimentally and theoretically, will allow for the evaluation of the potential of these membranes in biogas upgrading and other environmental applications.

**Author Contributions:** A.F.-B. performed the experimental work. C.C.-C. conceived, analyzed and wrote the first draft of the manuscript. A.I. provided the laboratory facilities and global analysis and feedback regarding the modeling validation. All authors have read and agreed to the published version of the manuscript.

**Funding:** This research was funded by the Spanish Ministry of Science, Innovation and Universities ([www.ciencia.gob.es](http://www.ciencia.gob.es)) under project CTQ2016-76231-C2-1-R.

**Conflicts of Interest:** The authors declare no conflict of interest. The funders had no role in the design of the study; in the collection, analyses, or interpretation of data; in the writing of the manuscript, or in the decision to publish the results.

## Abbreviations

<i>a</i>	water activity, in Equation (4)
A	Effective membrane area, cm <sup>2</sup>
β <sub>i</sub>	Intrinsic gas pair selectivity
CHF	Composite hollow fiber
CS	Chitosan biopolymer
Δ <i>p</i> <sub><i>i</i></sub>	partial pressure difference for the gas component <i>i</i>
D	Diffusivity, cm <sup>2</sup> s <sup>-1</sup> , in Equation (4)
FFV	Fraction of free volume
GPU	Units of permeance, 10 <sup>-6</sup> cm <sup>3</sup> (STP)·cm <sup>-2</sup> s <sup>-1</sup> cmHg <sup>-1</sup>
IL	Ionic liquid; in this work, 1-ethyl-3-methylimidazolium acetate
MMCHF	Mixed matrix composite hollow fiber
P84	BTDA-TDI/MDI, 3,3',4,4'-benzophenone tetracarboxylic dianhydride and 80% methylphenylene-diamine + 20% methylene diamine copolyimide
PSf	Polysulfone polymer
PTMSP	Poly[1-(trimethylsilyl)-1-propyne]
Q	Gas flow rate, cm <sup>3</sup> s <sup>-1</sup>
<i>t</i>	selective layer thickness
RH	Relative Humidity, %
S	Solubility, cm <sup>3</sup> (STP) cm <sup>-3</sup> ·g, in Equation (4)

## References

1. Merkel, T.C.; Zhou, M.; Baker, R.W. Carbon dioxide capture with membranes at an IGCC power plant. *J. Membr. Sci.* **2012**, *389*, 441–450. [[CrossRef](#)]
2. Luis, P.; Van der Bruggen, B. The role of membranes in post-combustion CO<sub>2</sub> capture. *Greenh. Gases Sci. Technol.* **2013**, *3*, 318–337. [[CrossRef](#)]
3. Basu, S.; Khan, A.L.; Cano-odena, A. Membrane-based technologies for biogas separations. *Chem. Soc. Rev.* **2010**, 750–768. [[CrossRef](#)] [[PubMed](#)]
4. Zhang, Y.; Sunarso, J.; Liu, S.; Wang, R. Current status and development of membranes for CO<sub>2</sub>/CH<sub>4</sub> separation: A review. *Int. J. Greenh. Gas. Control.* **2013**, *12*, 84–107. [[CrossRef](#)]

5. Scholes, C.A.; Stevens, G.W.; Kentish, S.E. Membrane gas separation applications in natural gas processing. *Fuel* **2012**, *96*, 15–28. [[CrossRef](#)]
6. Adewole, J.K.; Ahmad, A.L.; Ismail, S.; Leo, C.P. Current challenges in membrane separation of CO<sub>2</sub> from natural gas: A review. *Int. J. Greenh. Gas. Control.* **2013**, *17*, 46–65. [[CrossRef](#)]
7. Park, H.B.; Kamcev, J.; Robeson, L.M.; Elimelech, M.; Freeman, B.D. Maximizing the right stuff: The trade-off between membrane permeability and selectivity. *Science* **2017**, *356*, 1138–1148. [[CrossRef](#)]
8. Scholes, C.A.; Stevens, G.W.; Kentish, S.E. The effect of hydrogen sulfide, carbon monoxide and water on the performance of a PDMS membrane in carbon dioxide/nitrogen separation. *J. Membr. Sci.* **2010**, *350*, 189–199. [[CrossRef](#)]
9. Casado-Coterillo, C. Mixed matrix membranes. *Membranes* **2019**, *9*, 149. [[CrossRef](#)]
10. Dai, Z.; Ansaloni, L.; Deng, L. ScienceDirect Recent advances in multi-layer composite polymeric membranes for CO<sub>2</sub> separation: A review. *Green Energy Env.* **2016**, *1*, 102–128. [[CrossRef](#)]
11. Monsalve-Bravo, G.M.; Bhatia, S.K. Comparison of hollow fiber and flat mixed-matrix membranes: Theory and simulation. *Chem. Eng. Sci.* **2018**, *187*, 174–188. [[CrossRef](#)]
12. Vu, D.Q.; Koros, W.J.; Miller, S.J. Mixed matrix membranes using carbon molecular sieves: I. Preparation and experimental results. *J. Membr. Sci.* **2003**, *211*, 311–334. [[CrossRef](#)]
13. Zhang, C.; Zhang, K.; Xu, L.; Labreche, Y.; Kraftschik, B.; Koros, W.J. Highly scalable ZIF-based mixed-matrix hollow fiber membranes for advanced hydrocarbon separations. *AIChE J.* **2014**, *60*, 2625–2635. [[CrossRef](#)]
14. He, T.; Mulder, M.H.V.; Strathmann, H.; Wessling, M. Preparation of composite hollow fiber membranes: Co-extrusion of hydrophilic coatings onto porous hydrophobic support structures. *J. Membr. Sci.* **2002**, *207*, 143–156. [[CrossRef](#)]
15. Wang, B.; Sun, C.; Li, Y.; Zhao, L.; Ho, W.S.W.; Dutta, P.K. Rapid synthesis of faujasite/polyethersulfone composite membrane and application for CO<sub>2</sub>/N<sub>2</sub> separation. *Microporous Mesoporous Mater.* **2015**, *208*, 72–82. [[CrossRef](#)]
16. Khulbe, K.C.; Matsuura, T.; Feng, C.Y.; Ismail, A.F. Recent development on the effect of water/moisture on the performance of zeolite membrane and MMMs containing zeolite for gas separation; Review. *RSC Adv.* **2016**, *6*, 42943–42961. [[CrossRef](#)]
17. Li, P.; Chen, H.Z.; Chung, T.S. The effects of substrate characteristics and pre-wetting agents on PAN-PDMS composite hollow fiber membranes for CO<sub>2</sub>/N<sub>2</sub> and O<sub>2</sub>/N<sub>2</sub> separation. *J. Membr. Sci.* **2013**, *434*, 18–25. [[CrossRef](#)]
18. Pourafshari Chenar, M.; Soltanieh, M.; Matsuura, T.; Tabe-Mohammadi, A.; Khulbe, K.C. The effect of water vapor on the performance of commercial polyphenylene oxide and Cardo-type polyimide hollow fiber membranes in CO<sub>2</sub>/CH<sub>4</sub> separation applications. *J. Membr. Sci.* **2006**, *285*, 265–271. [[CrossRef](#)]
19. Wang, B.; Dutta, P.K. Influence of Cross-Linking, Temperature, and Humidity on CO<sub>2</sub>/N<sub>2</sub> Separation Performance of PDMS Coated Zeolite Membranes Grown within a Porous Poly(ether sulfone) Polymer. *Ind. Eng. Chem. Res.* **2017**, *56*, 6065–6077. [[CrossRef](#)]
20. Fam, W.; Mansouri, J.; Li, H.; Hou, J.; Chen, V. Gelled graphene oxide-ionic liquid composite membranes with enriched ionic liquid surfaces for improved CO<sub>2</sub> separation. *ACS Appl. Mater. Interfaces* **2018**, *10*, 7389–7400. [[CrossRef](#)]
21. Fernández-Barquín, A.; Rea, R.; Venturi, D.; Giacinti-Baschetti, M.; De Angelis, M.G.; Casado-Coterillo, C.; Irabien, Á. Effect of relative humidity on the gas transport properties of zeolite A/PTMSP mixed matrix membranes. *RSC Adv.* **2018**, *8*, 3536–3546. [[CrossRef](#)]
22. Yoo, M.J.; Lee, J.H.; Yoo, S.Y.; Oh, J.Y.; Roh, J.M.; Grasso, G.; Lee, J.H.; Lee, D.; Oh, W.J.; Yeo, J.-G.; et al. Defect control for large-scale thin-film composite membrane and its bench-scale demonstration. *J. Membr. Sci.* **2018**, *566*, 374–382. [[CrossRef](#)]
23. Chen, H.Z.; Thong, Z.; Li, P.; Chung, T.S. High performance composite hollow fiber membranes for CO<sub>2</sub>/H<sub>2</sub> and CO<sub>2</sub>/N<sub>2</sub> separation. *Int. J. Hydrogen Energy* **2014**, *39*, 5043–5053. [[CrossRef](#)]
24. Wang, Y.; Hu, T.; Li, H.; Dong, G.; Wong, W.; Chen, V. Enhancing membrane permeability for CO<sub>2</sub> capture through blending commodity polymers with selected PEO and PEO-PDMS copolymers and composite hollow fibres. *Energy Procedia* **2014**, *63*, 202–209. [[CrossRef](#)]
25. Li, T.; Pan, Y.; Peinemann, K.V.; Lai, Z. Carbon dioxide selective mixed matrix composite membrane containing ZIF-7 nano-fillers. *J. Membr. Sci.* **2013**, *425–426*, 235–242. [[CrossRef](#)]

26. Kouketsu, T.; Duan, S.; Kai, T.; Kazama, S.; Yamada, K. PAMAM dendrimer composite membrane for CO<sub>2</sub> separation: Formation of a chitosan gutter layer. *J. Membr. Sci.* **2007**, *287*, 51–59. [[CrossRef](#)]
27. Aroon, M.A.; Ismail, A.F.; Montazer-Rahmati, M.M.; Matsuura, T. Effect of chitosan as a functionalization agent on the performance and separation properties of polyimide/multi-walled carbon nanotubes mixed matrix flat sheet membranes. *J. Membr. Sci.* **2010**, *364*, 309–317. [[CrossRef](#)]
28. Fernández-Barquín, A.; Casado-Coterillo, C.; Palomino, M.; Valencia, S.; Irabien, A. LTA/Poly(1-trimethylsilyl-1-propyne) Mixed-Matrix Membranes for High-Temperature CO<sub>2</sub>/N<sub>2</sub> Separation. *Chem. Eng. Technol.* **2015**, *38*, 658–666. [[CrossRef](#)]
29. Casado-Coterillo, C.; Fernández-Barquín, A.; Zornoza, B.; Téllez, C.; Coronas, J.; Irabien, Á. Synthesis and characterisation of MOF/ionic liquid/chitosan mixed matrix membranes for CO<sub>2</sub>/N<sub>2</sub> separation. *RSC Adv.* **2015**, *5*, 102350–102361. [[CrossRef](#)]
30. Fernández-Barquín, A.; Casado-Coterillo, C.; Etxeberria-Benavides, M.; Zuñiga, J.; Irabien, A. Comparison of flat and hollow fiber mixed matrix composite membranes for CO<sub>2</sub> separation with temperature. *Chem. Eng. Technol.* **2017**, *40*, 997–1007. [[CrossRef](#)]
31. Fernández-Barquín, A.; Casado-Coterillo, C.; Irabien, Á. Separation of CO<sub>2</sub>-N<sub>2</sub> gas mixtures: Membrane combination and temperature influence. *Sep. Purif. Technol.* **2017**, *188*, 197–205. [[CrossRef](#)]
32. Lasseguette, E.; Carta, M.; Brandani, S.; Ferrari, M.C. Effect of humidity and flue gas impurities on CO<sub>2</sub> permeation of a polymer of intrinsic microporosity for post-combustion capture. *Int. J. Greenh. Gas. Control.* **2016**, *50*, 93–99. [[CrossRef](#)]
33. Wu, D.; Han, Y.; Salim, W.; Chen, K.K.; Li, J.; Ho, W.S.W. Hydrophilic and morphological modification of nanoporous polyethersulfone substrates for composite membranes in CO<sub>2</sub> separation. *J. Membr. Sci.* **2018**, *565*, 439–449. [[CrossRef](#)]
34. Scholes, C.A.; Chen, G.Q.; Lu, H.T.; Kentish, S.E. Crosslinked PEG and PEBAX membranes for concurrent permeation of water and carbon dioxide. *Membranes* **2015**, *6*, 1–10. [[CrossRef](#)]
35. Ahmad, N.N.R.; Leo, C.P.; Mohammad, A.W.; Ahmad, A.L. Interfacial sealing and functionalization of polysulfone/SAPO-34 mixed matrix membrane using acetate-based ionic liquid in post-impregnation for CO<sub>2</sub> capture. *Sep. Purif. Technol.* **2018**, *197*, 439–448. [[CrossRef](#)]
36. Lee, S.; Binns, M.; Lee, J.H.; Moon, J.H.; Yeo, J.G.; Yeo, Y.K.; Lee, Y.M.M.; Kim, J.K. Membrane separation process for CO<sub>2</sub> capture from mixed gases using TR and XTR hollow fiber membranes: Process modeling and experiments. *J. Membr. Sci.* **2017**, *541*, 224–234. [[CrossRef](#)]
37. Ahmad, F.; Lau, K.K.; Lock, S.S.M.; Rafiq, S.; Khan, A.U.; Lee, M. Hollow fiber membrane model for gas separation: Process simulation, experimental validation and module characteristics study. *J. Ind. Eng. Chem.* **2015**, *21*, 1246–1257. [[CrossRef](#)]
38. Henis, J.M.S.; Tripodi, M.K. Composite Hollow Fiber Membranes For Gas Separation: The Resistance Model Approach. In *Polymer Science and Technology*; Elsevier: Amsterdam, The Netherlands, 1982; Volume 16, pp. 75–78.
39. Kattula, M.; Ponnuru, K.; Zhu, L.; Jia, W.; Lin, H.; Furlani, E.P. Designing ultrathin film composite membranes: The impact of a gutter layer. *Sci. Rep.* **2015**, *5*, 15016. [[CrossRef](#)]
40. Minelli, M.; Sarti, G.C. Elementary prediction of gas permeability in glassy polymers. *J. Membr. Sci.* **2017**, *521*, 73–83. [[CrossRef](#)]
41. Olivieri, L.; Tena, A.; Grazia, M.; Angelis, D.; Hern, A.; Lozano, A.E.; Cesare, G. The effect of humidity on the CO<sub>2</sub>/N<sub>2</sub> separation performance of copolymers based on hard polyimide segments and soft polyether chains: Experimental and modeling. *Green Energy Env.* **2016**, *1*, 201–210. [[CrossRef](#)]
42. Lasseguette, E.; Rouch, J.C.; Remigy, J.C. Hollow-fiber coating: Application to preparation of composite hollow-fiber membrane for gas separation. *Ind. Eng. Chem. Res.* **2013**, *52*, 13146–13158. [[CrossRef](#)]
43. Liu, L.; Chakma, A.; Feng, X. Gas permeation through water-swollen hydrogel membranes. *J. Membr. Sci.* **2008**, *310*, 66–75. [[CrossRef](#)]
44. Kudasheva, A.; Sorribas, S.; Zornoza, B.; Téllez, C.; Coronas, J. Pervaporation of water/ethanol mixtures through polyimide based mixed matrix membranes containing ZIF-8, ordered mesoporous silica and ZIF-8-silica core-shell spheres. *J. Chem. Technol. Biotechnol.* **2015**, *90*, 669–677. [[CrossRef](#)]
45. Casado-Coterillo, C.; López-Guerrero, M.M.; Irabien, A. Synthesis and characterisation of ETS-10/acetate-based ionic liquid/chitosan mixed matrix membranes for CO<sub>2</sub>/N<sub>2</sub> permeation. *Membranes* **2014**, *4*, 287–401. [[CrossRef](#)]

46. Hu, L.; Cheng, J.; Li, Y.; Liu, J.; Zhang, L.; Zhou, J.; Cen, K. Composites of ionic liquid and amine-modified SAPO 34 improve CO<sub>2</sub> separation of CO<sub>2</sub>-selective polymer membranes. *Appl. Surf. Sci.* **2017**, *410*, 249–258. [[CrossRef](#)]
47. Brunetti, A.; Cersosimo, M.; Sung, J.; Dong, G.; Fontananova, E.; Moo, Y.; Drioli, E.; Barbieri, G. Thermally rearranged mixed matrix membranes for CO<sub>2</sub> separation: An aging study. *Int. J. Greenh. Gas. Control.* **2017**, *61*, 16–26. [[CrossRef](#)]
48. Golemme, G.; Policicchio, A.; Sardella, E.; De Luca, G.; Russo, B.; Liguori, P.F.; Melicchio, A.; Agostino, R.G. Surface modification of molecular sieve fillers for mixed matrix membranes. *Colloids Surf. A Phys. Eng. Asp.* **2018**, *538*, 333–342. [[CrossRef](#)]
49. Jusoh, N.; Lau, K.K.; Shariff, A.M.; Yeong, Y.F. Capture of bulk CO<sub>2</sub> from methane with the presence of heavy hydrocarbon using membrane process. *Int. J. Greenh. Gas. Control.* **2014**, *22*, 213–222. [[CrossRef](#)]
50. Ismail, A.F.; Lorna, W. Penetrant-induced plasticization phenomenon in glassy polymers for gas separation membrane. *Sep. Purif. Technol.* **2002**, *27*, 173–194. [[CrossRef](#)]
51. Wind, J.D.; Staudt-Bickel, C.; Paul, D.R.; Koros, W.J. The effects of crosslinking chemistry on CO<sub>2</sub> plasticization of polyimide gas separation membranes. *Ind. Eng. Chem. Res.* **2002**, *41*, 6139–6148. [[CrossRef](#)]
52. Santaniello, A.; Golemme, G. Interfacial control in perfluoropolymer mixed matrix membranes for natural gas sweetening. *J. Ind. Eng. Chem.* **2018**, *60*, 169–176. [[CrossRef](#)]
53. Casado-Coterillo, C.; Fernández-Barquín, A.; Valencia, S.; Irabien, A. Estimating CO<sub>2</sub>/N<sub>2</sub> permselectivity through Si/Al = 5 small-pore zeolites/PTMSP mixed matrix membranes: Influence of temperature and topology. *Membranes* **2018**, *8*, 32. [[CrossRef](#)]



© 2019 by the authors. Licensee MDPI, Basel, Switzerland. This article is an open access article distributed under the terms and conditions of the Creative Commons Attribution (CC BY) license (<http://creativecommons.org/licenses/by/4.0/>).